APPLIED GEOPHYSICS, Vol.13, No.2 (June 2016), P. 307-314, 9 Figures.
DOI:10.1007/s11770-016-0559-8

Seismic dynamic monitoring in CO_2 flooding based on characterization of frequency-dependent velocity factor*

Zhang Jun-Hua♦[1,2], Li Jun[1,2], Xiao Wen[1,2], Tan Ming-You[3], Zhang Yun-Ying[3], Cui Shi-Ling[3], and Qu Zhi-Peng[3]

Abstract: The phase velocity of seismic waves varies with the propagation frequency, and thus frequency-dependent phenomena appear when CO_2 gas is injected into a reservoir. By dynamically considering these phenomena with reservoir conditions it is thus feasible to extract the frequency-dependent velocity factor with the aim of monitoring changes in the reservoir both before and after CO_2 injection. In the paper, we derive a quantitative expression for the frequency-dependent factor based on the Robinson seismic convolution model. In addition, an inversion equation with a frequency-dependent velocity factor is constructed, and a procedure is implemented using the following four processing steps: decomposition of the spectrum by generalized S transform, wavelet extraction of cross-well seismic traces, spectrum equalization processing, and an extraction method for frequency-dependent velocity factor based on the damped least-square algorithm. An attenuation layered model is then established based on changes in the *Q* value of the viscoelastic medium, and spectra of migration profiles from forward modeling are obtained and analyzed. Frequency-dependent factors are extracted and compared, and the effectiveness of the method is then verified using a synthetic data. The frequency-dependent velocity factor is finally applied to target processing and oil displacement monitoring based on real seismic data obtained before and after CO_2 injection in the G89 well block within Shengli oilfield. Profiles and slices of the frequency-dependent factor determine its ability to indicate differences in CO_2 flooding, and the predicting results are highly consistent with those of practical investigations within the well block.
Keywords: CO_2 flooding, Frequency-dependent velocity factor, G89 well block, Reservoir dynamic monitoring

Introduction

Carbon dioxide (CO_2) flooding is an effective method whereby CO_2 is injected into a production well to displace oil and improve recovery. It is more effective and cheaper to use than using traditional water and steam flooding methods and is also beneficial in sequestering

Manuscript received by the Editor on January 13, 2016; revised manuscript received May 25, 2016.
*This work was supported by the Pilot Project of Sinopec (P14085).
1. School of Geosciences, China University of Petroleum, Qingdao 266580, China.
2. Laboratory for Marine Mineral Resources, Qingdao National Laboratory for Marine Science and Technology, Qingdao 266071, China.
3. Geophysical Research Institute of Shengli Oilfield Branch Company, Sinopec, Dongying 257015, China.
♦Corresponding author: Zhang Jun-Hua (Email: zjh_upc@163.com)

carbon. Seismic dynamic monitoring of CO_2 flooding is based on a time-lapse mode and is currently the focus of significant scientific attention. The seismic response obtained can be used to determine certain parameters such as characterize changes in reservoir fluid, track the front edge of fluid, determine CO_2 distribution, and determine the possibility of gas channeling and leakage. The use of time-lapse seismic response during oil and gas field development can thus determine the distribution of oil, gas, and water, and predict the amount of residual oil.

Recent research in this respect is listed as follows. Pawar et al. (2006) monitored the distribution of CO_2 at a depth of 1.4 km, thereby verifying the effectiveness of time-lapse seismic monitoring for CO_2 flooding. Monea et al. (2009) applied time-lapse seismic monitoring to Sleipner oilfield, where application results clearly showed a variety of shapes relating to the migration and distribution of oil caused by supercritical CO_2 in the salt-water reservoir; this study provided more powerful proof of the effectiveness of seismic dynamic monitoring during CO_2 flooding. Davis (2010) showed the occurrence of S-wave amplitude attenuation phenomenon during time-lapse seismic monitoring of the Weybern oilfield, and determined that this phenomenon was caused by an increase in fluid pressure in relation to CO_2 injection. At present, domestic research in CO_2 flooding is focused on injection production technology. However, in relation to an acceleration of energy-saving and emission-reduction policies, the use of seismic dynamic monitoring in CO_2 flooding is also beginning to receive increasing attention.

Velocity dispersion is the phenomenon whereby there is a change in the frequency of a seismic wave's phase velocity within a fluid medium. In recent years, a large amount of global research has been conducted on the interpretation and application of frequency-dependent attributes determined from seismic data. For example, Taner et al. (1979) discovered a "low-frequency shadow" under a reservoir when conducting complex seismic analysis. Castagna et al. (2003) used a high resolution spectral analysis method to study the low-frequency shadow phenomenon related to hydrocarbon in a reservoir, and a frequency-dependent AVO inversion was proposed to extract the quantitative form of frequency dependent attributes for a frequency-dependent case. In addition, Sun et al. (2013) and Lin et al. (2014) studied the relationship between fluid parameters and frequency and the influence law of seismic wave attenuation and dispersion. Wilson et al. (2009) studied Chapman's physical model of multiscale rock dispersion, and combined pre-stack inversion with the modern spectrum decomposition method; they finally proposed quantitative characterization methods for frequency dependent factors based on frequency dependent AVO inversion. Furthermore, Wu et al. (2010) combined the rearrangement of a high-resolution RSPWVD algorithm to achieve the frequency dependent AVO inversion method. Following this, Zhang et al. (2011) developed a Bayesian post-stack seismic inversion method based on p-wave velocity frequency dependent attributes, and applied the frequency dependent attributes to fluid identification in actual seismic data. Zhang et al. (2013) then researched the frequency-dependent sensitivity of elastic parameters, and proposed fluid factor inversion method based on Russell's approximation formula.

Based on the above-mentioned previous studies and actual field characteristics, this paper applies frequency-dependent velocity factors to monitor the dynamic changes within a reservoir in relation to CO_2 flooding. Our method uses the frequency dependent factor to detect the route taken by CO_2 flooding, and ultimately predicts the range of influence. Construction of a theoretical model and field case studies show that the frequency-dependent factors in our work are able to effectively detect reservoir anomalies. It is considered that the proposed method will have profound significance and application value for guiding reservoir dynamic monitoring and oil recovery enhancement.

Theory and method

If we consider the frequency-dependent phenomenon in the process of CO_2 flooding, the p-wave velocity, v_p, can be characterized as the function of frequency, $v_p(f)$. Therefore, the reflection coefficient can be written using the following form (Wilson et al., 2009; Zhang et al., 2011),

$$r(f)=\frac{v_{p2}(f)\rho_2-v_{p1}(f)\rho_1}{v_{p2}(f)\rho_2+v_{p1}(f)\rho_1}=\frac{1}{2}\left[\frac{\Delta v_p}{v_p}(f)+\frac{\Delta\rho}{\rho}\right], \quad (1)$$

where $r(f)$ is the reflection coefficient; v_{p1} and v_{p2} are the p-wave velocity of the upper and lower layers, respectively; ρ_1 and ρ_2 are the density of the upper layer and lower layer, respectively; Δv_p is the velocity difference of the upper and lower layer; and v_p and ρ

are the average p-wave velocity and average density, respectively.

From Robinson's stationary seismic convolution model, we can find that zero-offset seismic records are equivalent to convolution of the wavelet and reflection coefficient, and are also equivalent to the product of the reflectance spectrum and wavelet spectrum in the frequency domain as

$$r(\mathrm{t}, f) * w(\mathrm{t}, f) = s(\mathrm{t}, f), \quad (2)$$

where $s(t, f)$ represents the instantaneous spectrum of the seismic signal. As the seismic wavelet obscures information from the stratigraphic interface, it is necessary to broaden the seismic record spectrum to restore acoustic reflection information resulting from complex underground media. Therefore, assuming that reflectivity accords with the Gaussian distribution, the specific process of spectrum equalization can be expressed as

$$r(\mathrm{t}, f) = \frac{s(\mathrm{t}, f)}{w(\mathrm{t}, f) + \varepsilon}, \quad (3)$$

where ε is dimensionless and is mainly used to improve the stability of spectrum equalization. The Taylor expansion is used in the expression $r(t, f)$ at f_0, and if ignoring the higher order it yields

$$r(\mathrm{t}, f) \approx r(\mathrm{t}, f_0) + D_{Rf} * df, \quad (4)$$

where $D_{Rf} = \frac{\partial[r(\mathrm{t}, f)]}{\partial f}$ represents the frequency-dependent degree of reflectivity. Assuming that density does not vary with frequency (Wu et al., 2010), the partial derivative of density versus frequency is negligible, and thus equation (1) can be substituted into equation (4) as

$$r(t, f) - \frac{1}{2}R_\rho(t) = \frac{1}{2}\frac{\Delta v_p}{v_p}(f_0) + \frac{1}{2}D_{vf}\left(f - f_0\right), \quad (5)$$

where $R_p = \frac{\Delta v_p}{v_p}(f)$ is the reflectivity of p-wave velocity and $D_{vf} = \frac{\partial R_v}{\partial f}$ is the quantitative characterization form of the frequency-dependent degree. If we substitute equations (2) and (3) into equation (5), considering the N sampling points and M frequencies we obtain

$$\begin{bmatrix} \frac{\mathbf{s}(\mathrm{t}, f_1)}{w(\mathrm{t}, f_1) + \varepsilon} - \frac{1}{2}\mathbf{R}_\rho(f_0) \\ \frac{\mathbf{s}(\mathrm{t}, f_2)}{w(\mathrm{t}, f_2) + \varepsilon} - \frac{1}{2}\mathbf{R}_\rho(f_0) \\ \vdots \\ \frac{\mathbf{s}(\mathrm{t}, f_M)}{w(\mathrm{t}, f_M) + \varepsilon} - \frac{1}{2}\mathbf{R}_\rho(f_0) \end{bmatrix} = \begin{bmatrix} 0.5 * \mathbf{E} & (f_1 - f_0) * \mathbf{E} \\ 0.5 * \mathbf{E} & (f_2 - f_0) * \mathbf{E} \\ \vdots & \vdots \\ 0.5 * \mathbf{E} & (f_M - f_0) * \mathbf{E} \end{bmatrix} \begin{bmatrix} \mathbf{R}_{v0} \\ \mathbf{D}_{vf} \end{bmatrix}, \quad (6)$$

where $\mathbf{E}_{N*N}$ is the unit diagonal matrix, $\mathbf{R}_\rho$ is the column vector consisting of the density reflection coefficients, and $\mathbf{R}_{v0}$ is the value of the velocity reflection coefficient at a reference frequency, f_0. To simplify the inversion problem, we let **Y** represent the actual seismic reflection response, **F** represent the core matrix of the inversion process, and **X** represent the parameter of the inversion process (which we will extract). This article uses the damped least square method to solve this equation, and as such the equation is expressed as

$$\mathbf{X} = (\mathbf{F}^{-1} * \mathbf{F} + \varepsilon_0{}^2\mathbf{E})^{-1} * \mathbf{Y}. \quad (7)$$

It is necessary to combine the S transform in the extraction process of frequency-dependent factors, and the specific processing steps involved include the following. 1) Utilizing the generalized S transform spectrum decomposition to extract several single frequency profiles before and after CO_2 injection. 2) Time-frequency analysis of the seismic trace before and after CO_2 injection, and synthesizing the logging curve and borehole-side trace to extract the seismic wavelet. 3) Spectrum equalization processing of time-lapse seismic data to enable removal of “wavelet fold-over” influence and restore stratum reflectivity of frequency-dependent response. 4) Furthermore, according to the extraction equation of frequency-dependent factors, profiles of the frequency-dependent factors can be extracted based on the damped least-square method.

Synthetic test

Model establishment

To verify feasibility of the proposed method, synthetic gathers were generated using the forward modeling method in a viscoelastic medium to simulate dispersion and attenuation caused by the CO_2 injection (Carcione et al., 1988). Because of the computing efficiency of the numerical simulation and the programming complexity, this paper uses the Kelvin-Voight model. The viscoelastic equation related to this model can be expressed as (Sun and Li, 2011)

$$\frac{1}{\rho(x)}\frac{\partial p}{\partial t}=-V(x)^2\left[\frac{\partial v}{\partial x}+\frac{\partial u}{\partial z}\right]-V^*(x)^2\left[\frac{\partial^2 v}{\partial x\partial t}+\frac{\partial^2 u}{\partial z\partial t}\right],$$
$$\frac{\partial v}{\partial t}=-\frac{1}{\rho(x)}\frac{\partial p}{\partial x},$$
$$\frac{\partial u}{\partial t}=-\frac{1}{\rho(x)}\frac{\partial p}{\partial z}, \tag{8}$$

where p is the unit diagonal matrix, v and u are the horizontal and vertical component of particle vibration, respectively. $\rho(x)$ is the density, $V(x)$ is the P-velocity, $V^*(x)^2=\frac{V(x)^2}{Q\omega_0}$, Q represents the quality factor, ω_0 is the reference frequency. Figure 1 shows a theoretical model of the viscoelastic medium. We assumed that there was no change in reservoir thickness either before or after CO_2 injection and ignored the effect of a thin inter-bed on the tuning frequency. It is evident that differences in seismic attenuation are represented by various quality factors, Q, which represent the process of CO_2 flooding (as shown in the third layer of Figure 1 where values of Q on the left and right sides are 20 and 200, respectively). The model is composed of 1201-by-400 grids with a space interval of 5 m in both the horizontal and vertical directions, and the first shot is located at grid point (201, 0). There are 401 receivers evenly spaced along the surface on two sides of the source, with a receiver interval of 20 m between each. The staggered-grid finite difference scheme was used for forward modeling, and to obtain seismic data of 181 shots we used the 10th-order staggered-grid finite difference scheme to generate seismic data. Figure 2 shows the results of post-stack migration using Kirchhoff migration.

Instantaneous spectral analysis

To clearly determine the frequency-dependent effect evoked by varying degrees of attenuation, this paper conducts an instantaneous spectral analysis using the times shown in the migration result of Figure 2. Figure 3a shows the time-frequency spectra corresponding to the upward, middle, and downward interfaces of CDP1000 and CDP150. It is evident that the frequency bandwidth of the first layer remains roughly the same, the middle layer decreases slightly, the attenuation value of low frequency is less than 1Hz, and that the bottom layer is noticeable, the attenuation value is about 7Hz (as shown

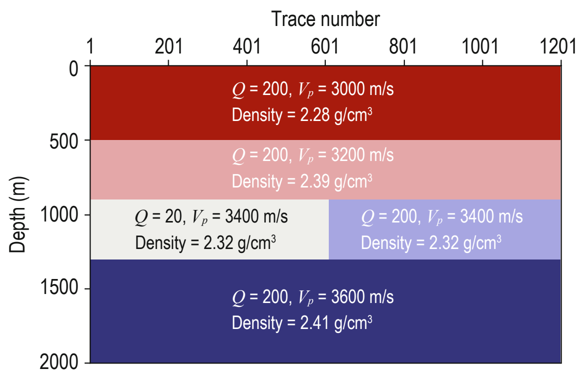

Fig.1 Theoretical model.

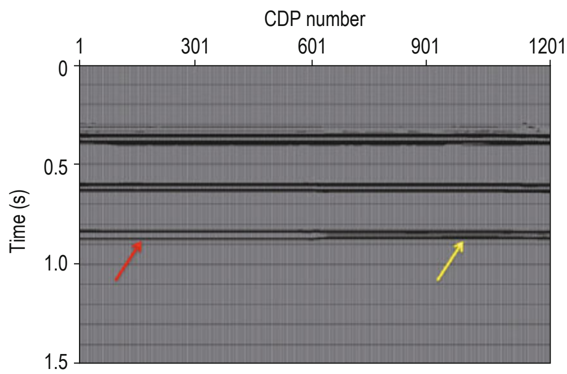

Fig.2 Migration result after precise processing.

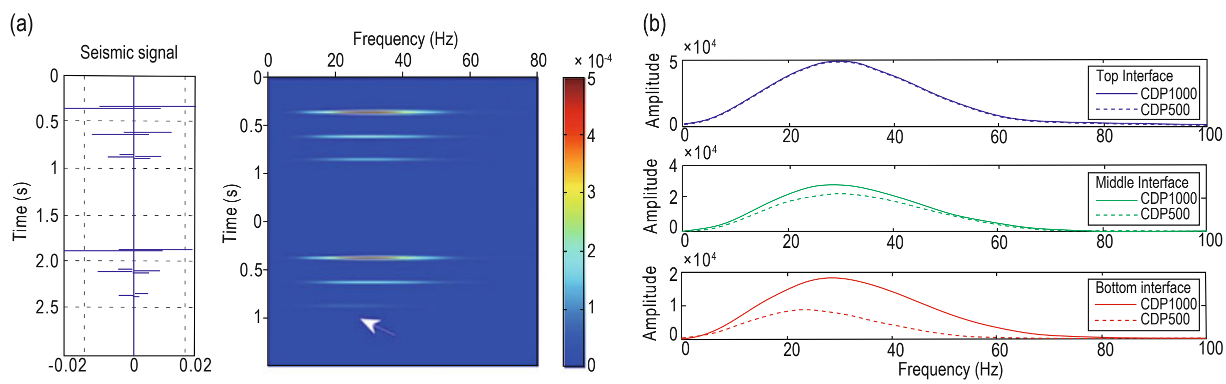

Fig.3 Time-frequency spectra corresponding to CDP1000 and CDP150.

by the in Figure 3a). As there are distinct differences between the frequency bandwidths, our method can thus be used to extract frequency-dependent factors, and we therefore extract the instantaneous spectral curve of bottom reflection. As shown in Figure 3b, the bandwidth of the bottom stratum is evidently reduced at the location of CDP150 compared with CDP1000 (the reference layer), and high frequency attenuation is obvious when the Q value is 20. These results thus lay the foundation for extracting seismic frequency-dependent factors.

Extraction and analysis of frequency-dependent factor

As the method we introduced in section "Synthetic test", the spectrum equalization should be done firstly, and the reference frequency f0 is 21 Hz, this frequency is also the main frequency of wavelet in the forward modelling. Then, we calculate the velocity frequency-dependent factor based on equation (6). Figure 4 shows the extracted result of P-velocity dispersion factors at locations of CDP150 and CDP1000, where the blue and red lines represent reference traces of CDP1000 and CDP150, respectively. We can see that P-velocity dispersion factors preserve a high degree of consistency at the top interface (no attenuation effect), but that there is a slight difference in the position of the middle interface. It is thus possible to conclude that the top reflection of the attenuation layer will also be affected by inner-layer attenuation. Furthermore, there is a larger difference in the bottom reflection of the attenuation layer compared with the reflection in the two layers above. Therefore, the frequency-dependent effects of reflection of the three layers are basically the same at the position of CDP1000, but the frequency-dependent factors increase gradually from the shallow to deep layers at the location of CDP150. All the synthetic tests therefore illustrate the feasibility of our method, and establish a solid foundation for the filed application.

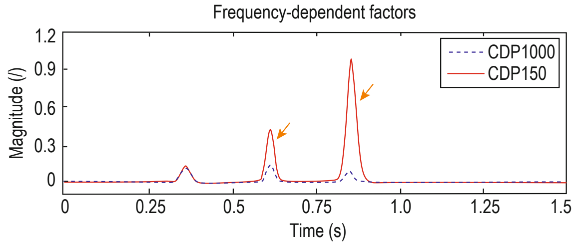

Fig.4 Estimated frequency-dependent factors.

Application in the field

Basic situation of well block

To demonstrate the effectiveness of our method in the field of reservoir dynamic monitoring, our method is applied to the G89 well block of Shengli oilfield in eastern China, which is the largest area use for experimental CO_2 flooding. Figures 5a–b show two seismic profiles across known wells before and after CO_2 injection, which were acquired in 1992 and 2011, respectively, where the data are consistent with respect to processing, amplitude, and time differences. In addition, the reference layer and the area that did not receive a gas injection also have good consistency, so it is therefore possible to rule out any changes caused by seismic data acquisition and processing parameters. The wells in which CO_2-injection occurred are G89-4 and G89-9 (gas injection occurred in 2008), and the production wells are G89-S3 and G891-7. Red ellipses indicate the position of the oil reservoir in our experimental area. CO_2 was injected into the reservoir in a liquid form at a reservoir depth of 3000 m. The pressure initially reached 40 MPa, but after CO_2 injection was 28.7 MPa; temperature was 126°, and CO_2 existed in

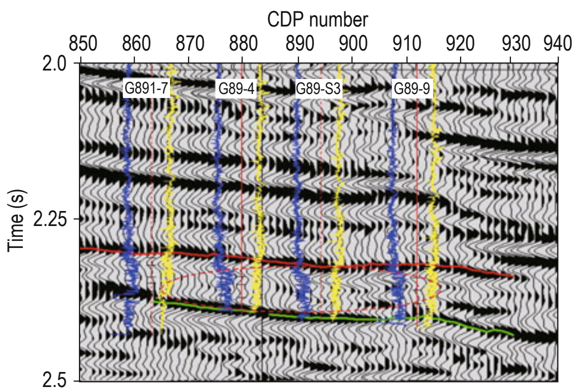

(a) Before CO_2 injection

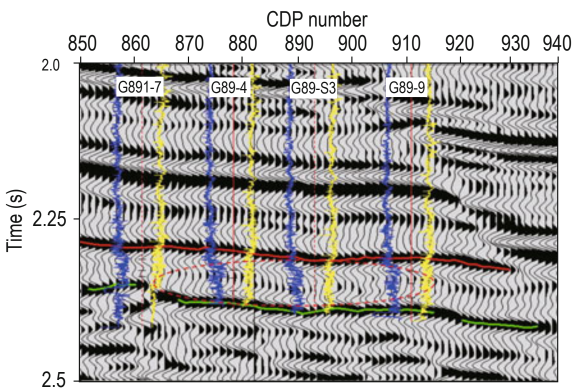

(b) After CO_2 injection

Fig.5 Field seismic profiles across known wells before and after CO_2 injection.

a gas-liquid form within the reservoir.

We initially conducted an instantaneous spectral analysis of the borehole-side traces, which assisted in determining the reference frequency for the inversion process.

Time-frequency spectra of borehole-side traces

The time-frequency spectra corresponding to borehole-side traces before and after CO_2 injection are shown in Figure 6, where high-frequency attenuation is more obvious than low-frequency at the location of gas injection in G89-4 well (rectangular boxes shown in Figure 6). In addition, there is an evident decrease in the band-width of the attenuation spectrum compared with the reference spectra. the bandwidth reduced about 8 Hz. .While this phenomenon is also seen in the production well (G89-S3), the bandwidth reduced about 14 Hz, these results give us a foundation for extracting frequency-dependent velocity factors.

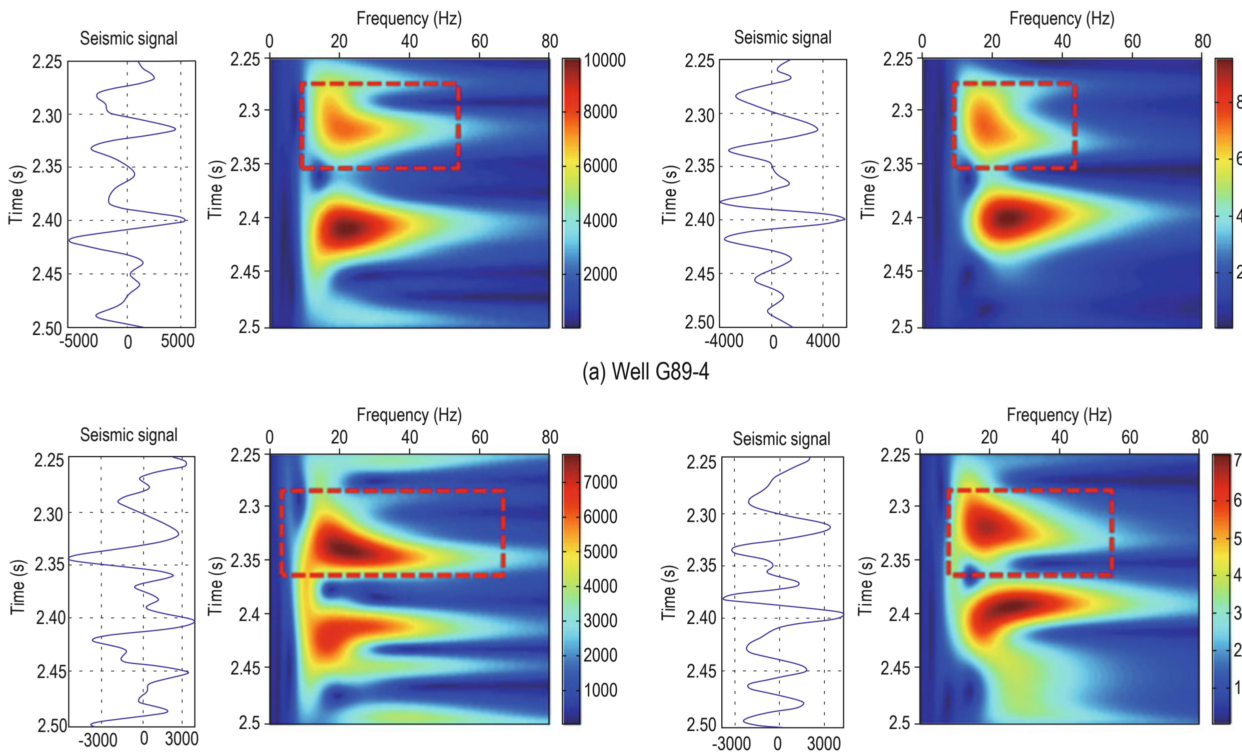

Fig.6 Time-frequency spectra of borehole-side traces before and after CO_2 injection.

Extraction of frequency-dependent factor and field verification

First of all, we extract the seismic wavelet by the comprehensive analysis of borehole-side trace and logging data, and the main frequency of wavelet is 21 Hz, this is also the reference frequency f0, then we do the spectrum equalization, finally we calculate the velocity frequency-dependent factor based on equation (6).

Figures 7a–b show extraction results of frequency-dependent velocity factors. A significant difference can be seen at the location of the reservoir with CO_2 flooding, where the frequency-dependent factors increase sharply in wells G89-4 and G89-9 due to the influence of CO_2 flooding. This result is consistent with the "low-frequency shadow" phenomenon occurring under the gas reservoir. However, frequency-dependent factors near production wells G89-S3 and G891-7 are also affected by CO_2 flooding, and these results indicate that the use of frequency-dependent factors can monitor the path of CO_2 flooding and predict its scope of dynamic influence.

Our method was then also applied to 3-D field data. Figure 8 shows the attribute slices of frequency-dependent factors, where red dots represent production wells and black dots represent CO_2 injection wells. As the frequency-dependent factors have high-value anomalies at the well block after CO_2 injection, it is therefore possible to effectively predict the area of CO_2 flooding influence.

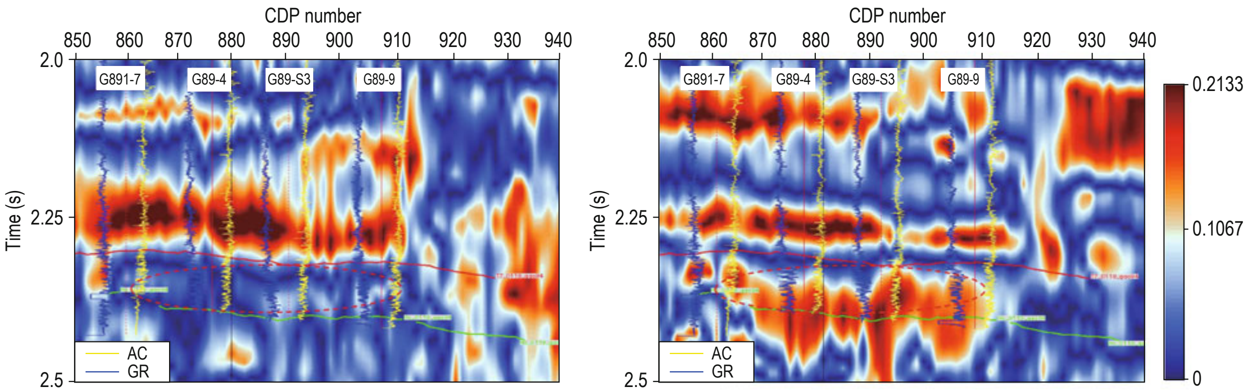

(a) Before CO_2 injection (b) After CO_2 injection

Fig.7 Extraction results of frequency-dependent velocity factors.

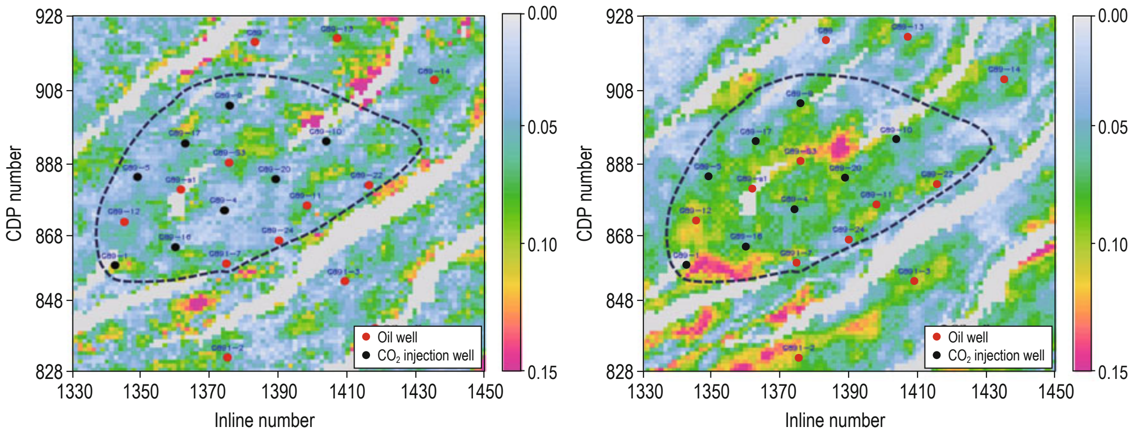

(a) Before CO_2 injection (b) After CO_2 injection

Fig.8 Slice analysis of frequency-dependent factors at top of reservoir.

To prove the validity of our method, we also performed field investigations at the well block. CO_2 was injected into certain wells (G89-4 etc.) in a liquid form (top right-hand photo of Figure 9). We observed the CO_2 gas outlet of the oil tank to determine whether the gas drive had reached the production wells (shown in the bottom right-hand photo of Figure 9). The results of predictions were highly correlated with the actual results determined from the 16 wells, as follows. 1) The 9 production wells in Figure 8 were found to emit CO_2 gas. 2) The gas drive had been sealed by the large, lower north-west fault causing it to stop within G891-3. 3) It was not possible to observe CO_2 gas in G89-14, as it was located deeply within the geological structure, but

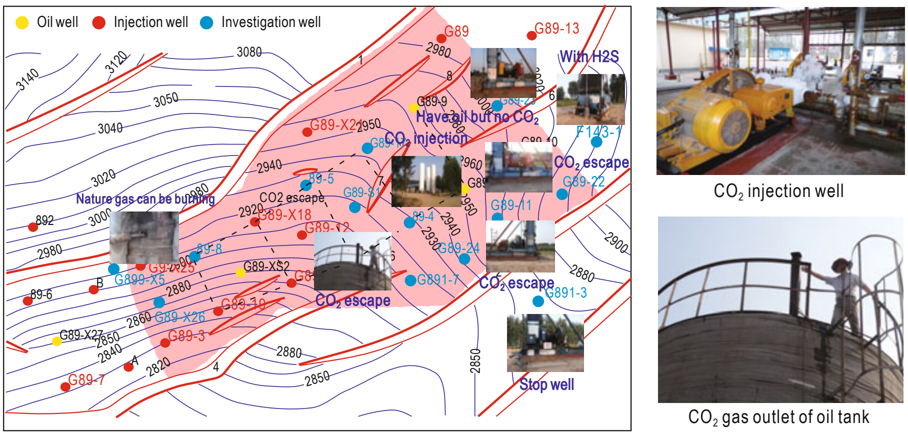

Fig.9 Field inspection of well block flooded with CO_2.

the smell of hydrogen sulfide gas was evident outside the wells, which illustrates that this wells is not under the area of influence of CO_2 flooding. 4) The geologic structure to the west of G89-1 is located at a high point. However, as the gas determined at the outlet could burn, it indicated that CO_2 flooding had not reached the structure. Further analysis concluded that the reservoir and injection were disconnected by a sand body.

Conclusions

Frequency-dependent phenomenon and amplitude attenuation are caused by CO_2 injection, and it is thus possible to use frequency-dependent velocity factors to monitor the dynamic characteristic of a reservoir. In this paper, the quantitative form of frequency-dependent factors were deduced based on the convolution model, and inversion equations containing frequency-dependent velocity factors were established. The feasibility of our method was verified using a synthetic attenuation test, and the method was then applied to oil displacement monitoring based on seismic data both before and after CO_2 injection in the G89 well block of Sheng-li oilfield in eastern China. Application of this method in the field shows that the frequency-dependent factors in our work can effectively detect reservoir anomalies both before and after CO_2 injection, and predict the influence of the area of CO_2 flooding. It is also considered that this work will be significant in guiding reservoir dynamic monitoring and oil recovery enhancement. However, this study shows that frequency-dependent velocity factor and other oil displacement monitoring methods need to be based on fine processing of seismic data, and that in this respect time and amplitude matching are extremely important.

Acknowledgements

We are grateful to our reviewers, Prof. Li Hui, Wang Yanchun, Ma Jinfeng, and Li Guofa, for their feedback that assisted in substantially improving the presentation of this paper.

References

Carcione, J. M., Kosloff, D., and Kosloff, R., 1988, Wave propagation simulation in a linear viscoacoustic medium: Geophysical Journal International, **93**(2), 393−401.

Castagna, J. P., Sun, S., and Siegfried, R. W., 2003, Instantaneous spectral analysis: Detection of low frequency shadows associated with hydrocarbons: The Leading Edge, **22**(2), 120–127.

Davis, T., 2010, The state of EOR with CO2 and associated seismic monitoring: The leading edge, **29**(1), 31–33.

Lin, K., He, Z. H., Xiong, X. J., et al., 2014, AVO forwarding modeling in two-phase media: multiconstrained matrix mineral modulus inversion: Applied Geophysics, **11**(4), 395–404.

Monea, M., Knudsen, R., Worth, K., et al., 2009, Considerations for monitoring, mitigation, and verification for GS of CO_2: Geophysical Monograph, **183**, 303–316.

Pawar, R., Lorenz, J., Byrer, C., et al., 2006, Sequestration of CO_2 in a depleted sandstone oil reservoir: results of a field demonstration test: 8th international conference on Greenhouse Gas Control technologies, Trondhein, Norway.

Sun, C. Y., and Li, Z. C., 2011, Foundation of seismic wave dynamics: Petroleum Industry Press, China, 178–182.

Sun, W. Y., Zhang, H. X., and Sun, Y., 2013, Apply S-transform to extract the attenuation and dispersion attributes of the seismic wave to detect Oil and Gas: Periodical of Ocean University of China, **43**(10), 83–87.

Taner, M. T., Koehler, F., and Sheriff, R., 1979, Complex seismic trace analysis: Geophysics, **44**(6), 1041–1063.

Wilson, A., Chapman, M., and Li, X. Y., 2009, Frequency-dependent AVO inversion: SEG Technical Program Expanded Abstracts, 341–345.

Wu, X., Chapman, M., Wilson, A., et al., 2010, Estimating seismic dispersion from pre-stack data using frequency dependent AVO inversion: SEG Technical Program Expanded Abstracts, 425–429.

Zhang, S. X., Yin X. Y., Zhang, G. Z., et al, 2011, Inversion method for the velocity dispersion-dependent attribute of P-wave: Geophysical Prospecting for Petroleum, **50**(3), 219–225.

Zhang, Z., Yin, X. Y., and Zong, Z. Y., 2013, A new frequency-dependent AVO attribute and its application in fluid identification: 75th EAGE Conference & Exhibition incorporating SPE EUROPEC, London, Britain.

Zhang Jun-Hua (Professor) gained a B.S. in Geophysical Prospecting in 1987, a M.S. in Geophysical Exploration and Information Technology in 1995, and a Ph.D. from the China University of Petroleum (East China) in 2002. He is currently at the School of Geosciences, China University of Petroleum (East China).